

Analysis of the structure, particle morphology and photoluminescent properties of green emitting $\text{BaB}_8\text{O}_{13}:\text{Ce}^{3+}$ phosphor

MA Lephoto¹, KG Tshabalala¹, SJ Motloun¹ and OM Ntwaeaborwa²

¹Department of Physics, University of the Free State (Qwa Qwa Campus), Private Bag X13, Phuthaditjhaba, 9866, South Africa

²School of physics, University of the Witwatersrand, Private Bag 3, Wits, 2050, South Africa

E-mail: ntwaeab@gmail.com

Abstract. $\text{BaB}_8\text{O}_{13}:\text{Ce}^{3+}$ powder phosphors were synthesized by the solution combustion method for general lighting applications. Powder X-ray diffraction pattern confirmed the formation of orthorhombic structure of $\text{BaB}_8\text{O}_{13}$ and the crystallite sizes estimated with Scherrer's equation and Hall-Williamson's plot were in the nanometre scale. Scanning electron microscopy micrographs showed that the particles have irregular shapes and were agglomerated together. The bands in the Fourier transform infrared spectra in the range of $650 - 1600 \text{ cm}^{-1}$ confirmed the formation of borate host. The $\text{BaB}_8\text{O}_{13}:\text{Ce}^{3+}$ powder phosphors showed emission at around 515 nm ascribed to the $5d^1 - 4f^1$ transition of Ce^{3+} after excitation at 270 nm using a monochromatized xenon lamp. A standard CIE diagram derived from relative emissions from the powder phosphors suggested a unique emission concentrated in the green region, thus the phosphor serve as a potential source of green light in light emitting devices.

1. Introduction

Oxide materials such as borate compounds are excellent hosts for luminescent dopant ions because of their good optical properties, such as high damage threshold and good non-linearity. They also have good chemical and thermal stability, low synthesis temperature and they can be synthesized cost effectively [1]. Barium octaborate $\text{BaB}_8\text{O}_{13}$ is considered as an excellent host material for luminescent dopant ions. Its structure consists of two separated interlocking three dimensional infinite network as alternating triborate and pentaborate groups, which forms BO_3 triangles and BO_4 tetrahedral units [2]. Ce^{3+} ions have been widely used as activators in various fluoride and oxide materials. The preparation of rare earth doped phosphor materials for application in advanced illumination technologies has been the subject of intense research for many decades. This type of research has been encouraged by the need to increase the efficiency of white light emitting solid state devices which can serve as an alternate source of lighting [3].

In most Ce^{3+} doped phosphors, parity allowed $5d - 4f$ emission ranging from ultra-violet to red color has been demonstrated and it is dependent on the host lattice and the site size, and the size symmetry and coordination number. In fact, the emission color of Ce^{3+} can be from the ultraviolet to visible region of the electromagnetic wave spectrum due to dependence of the $5d$ level of Ce^{3+} on the crystal field strength of the host lattice [4]. Different methods including wet chemistry and solid state

have been used to prepare different types of phosphors. Among these methods, the solution combustion has been widely used due to versatility, easy of incorporation of dopant ions, cost effectiveness and relatively short reaction time. Depending on the type of precursors, as well as conditions used for the process, the solution combustion may occur as either volume or layer-by-layer propagating combustion modes. This process may not only yield nanosized materials but also uniform (homogeneous) doping of traces of rare-earth impurity ions in a single step [5]. In the current study, $\text{BaB}_8\text{O}_{13}:\text{Ce}^{3+}$ powder phosphors were synthesized by the solution combustion method. The photoluminescent properties, structure and particle morphology of these phosphors are reported.

2. Experimental

Powder samples of $\text{BaB}_8\text{O}_{13}:x\text{Ce}^{3+}$ ($x = 0.03, 0.05, 0.07, 0.09$ and 0.11) were synthesized by a solution combustion method. The following precursors all in analytical purity were used: Barium nitrate [$\text{Ba}(\text{NO}_3)_2$], boric acid [H_3BO_3], Cerium nitrate [$\text{CeN}_3\text{O}_9 \cdot 6\text{H}_2\text{O}$], ammonium nitrate [NH_4NO_3] and urea [NH_2CONH_2]. In this preparation, NH_4NO_3 was used as an oxidizer and NH_2CONH_2 was used as a fuel. The stoichiometric amounts of reactants were mixed in a beaker with 10 mL of de-ionized water and stirred vigorously using a magnetic stirrer on a hot plate maintained at a temperature of 70°C for 30 min. The resulting solution was then transferred to a crucible and was introduced into a muffle furnace preheated to 600°C . Within a few minutes, the solution boiled and ignited to produce a self-propagating flame. The entire combustion process was complete in less than 5 min but the crucible was left in the furnace for 10 min to ensure that decomposition was complete. After 10 min the crucible was removed from the furnace and allowed to cool to room temperature. The combustion ashes of the powder samples were ground gently into fine powders using pestle and mortar. The powders were post annealed at 800°C for 5 hours in a muffle furnace. The structure, particle morphology and photoluminescent properties of the synthesized powder phosphors were examined by means of X-ray diffraction (XRD), Fourier transform spectroscopy (FTIR), scanning electron microscopy (SEM), Elemental energy dispersive analysis (EDS) and photoluminescence spectroscopy (PL emission and PL excitation).

3. Results and Discussion

Figure 1(a) shows the powder X-ray diffraction (XRD) patterns of $\text{BaB}_8\text{O}_{13}:x\text{Ce}^{3+}$ ($x = 0.03, 0.05, 0.07, 0.09$ and 0.11) powder phosphors. The XRD patterns of the powder phosphors were indexed to orthorhombic structure with cell parameters $a = 8.550 \text{ \AA}$, $b = 17.350 \text{ \AA}$ and $c = 13.211 \text{ \AA}$ according to JCPDS card no: 20-0097 [2]. The patterns show some extra peaks marked with asterisks (*) which may be attributed to the unreacted precursors during the combustion reaction. The presence of other phases or some of the precursors is attributed to the fact that the combustion wave is not uniform and portion of the precursors might not react completely during the combustion process [6]. The patterns also show a shift of peaks towards the lower angle as shown in figure 1(b). The observed XRD peak shifts might be caused by the lattice strain or lattice defects [7]. The average crystallite sizes of the phosphors were estimated by using Scherrer's equation [8]. The estimated average crystallite sizes of $\text{BaB}_8\text{O}_{13}:x\text{Ce}^{3+}$ powder phosphors were found to be 32, 36, 39, 43 and 40 nm for $x = 0.03, 0.05, 0.07, 0.09$ and 0.11 , respectively. The crystal structure of $\text{BaB}_8\text{O}_{13}$ host matrix is shown in figure 1(c). It is observed from the crystal structure that $\text{BaB}_8\text{O}_{13}$ consists of both tetrahedron (BO_4) and triangular (BO_3) groups. Looking at the ion bond between Ba, B and O ions, it is observed that B and Ba are connected via O ions. According to our calculations, the average bond lengths between B-O and Ba-O were 1.415 \AA and 2.713 \AA , respectively. The average bond angles between O-B-O, B-O-B and Ba-O-B were calculated to be 111.34° , 128.47° and 115.57° , respectively.

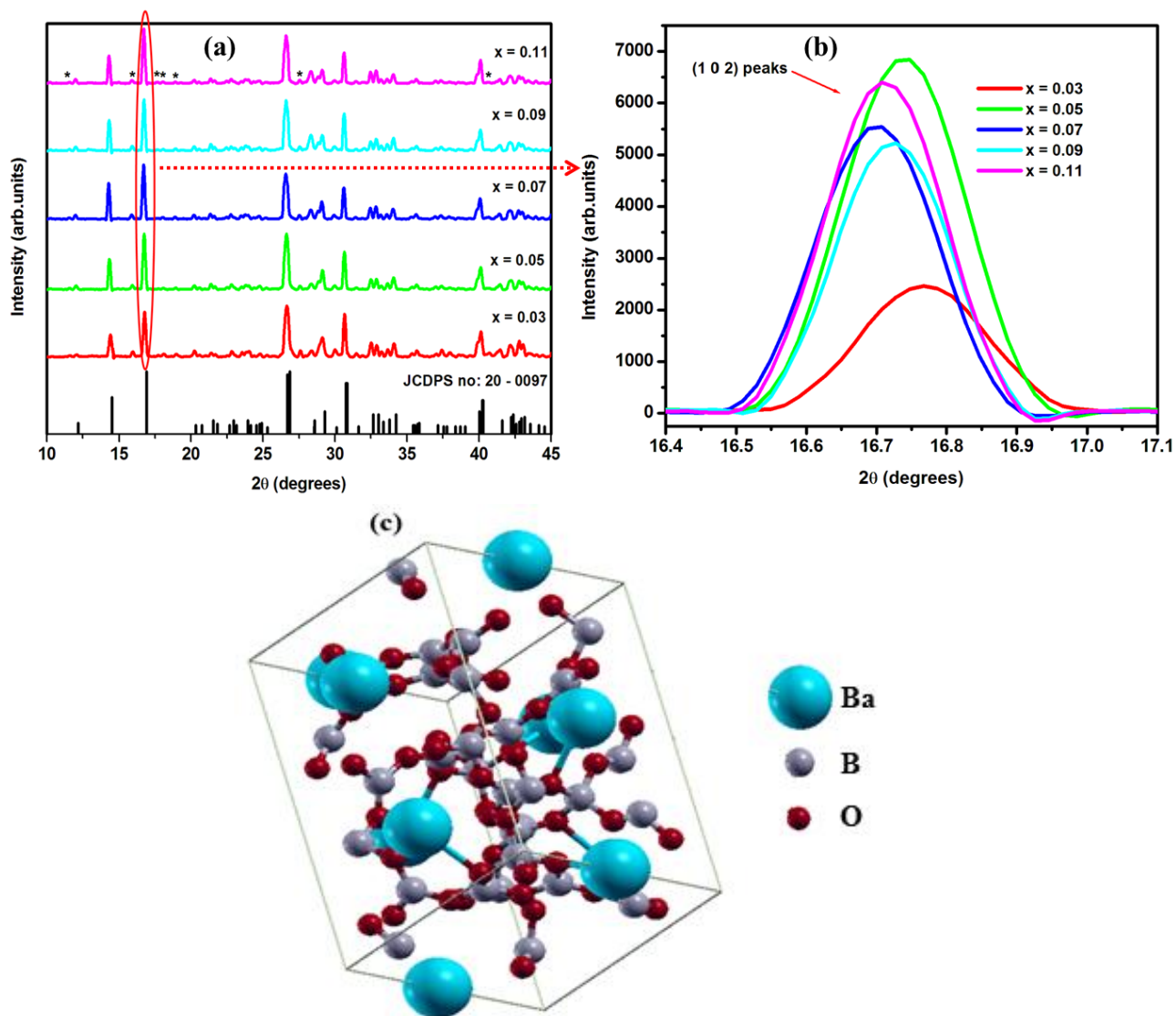


Figure 1. (a) Room temperature XRD pattern of $\text{BaB}_8\text{O}_{13}:x\text{Ce}^{3+}$ powder phosphors, (b) magnified view of (102) plane for $\text{BaB}_8\text{O}_{13}:x\text{Ce}^{3+}$ powder phosphors and (c) crystal structure of $\text{BaB}_8\text{O}_{13}$ host (blue, grey and red balls represent barium, boron and oxygen atoms, respectively).

Figure 2 shows the Fourier Transform Infrared (FTIR) spectrum of $\text{BaB}_8\text{O}_{13}:0.05\text{Ce}^{3+}$ powder phosphor. The FTIR spectrum was recorded in the spectral range of $650 - 3000 \text{ cm}^{-1}$. The spectrum exhibits some broad bands in the range $650 - 1600 \text{ cm}^{-1}$. The bands at $698, 730, 775,$ and 799 cm^{-1} are assigned to the out-of-plane bending mode of the group BO_3 . The in-plane bending modes of the BO_3 group are shown by the bands at $871, 928, 980, 1101$ and 1138 cm^{-1} . The bands peaking at $1235, 1270, 1319, 1363$ and 1408 cm^{-1} are assigned to the asymmetric stretching vibration of the BO_3 group [1].

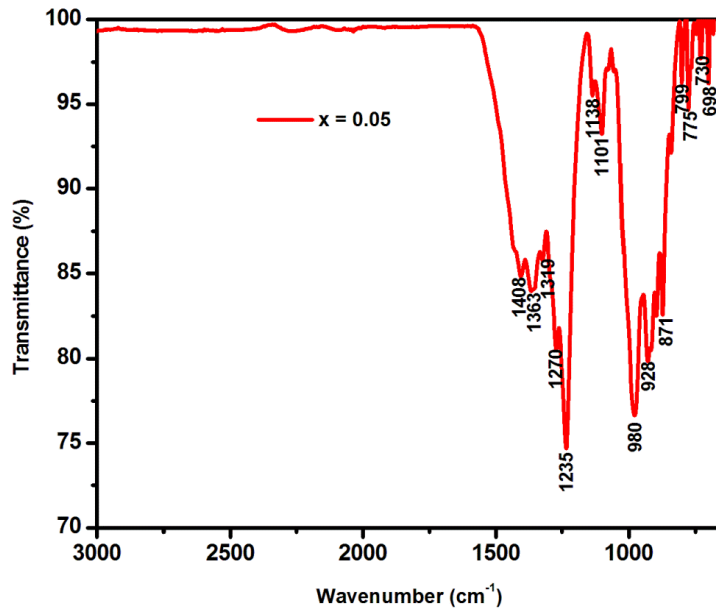


Figure 2. Room temperature FTIR spectrum of $\text{BaB}_8\text{O}_{13}:0.05\text{Ce}^{3+}$ phosphor.

The scanning electron microscope (SEM) micrograph of $\text{BaB}_8\text{O}_{13}:0.05\text{Ce}^{3+}$ powder phosphor taken at $\times 5000$ magnification is shown in figure 3(a). It is observed that the microstructures of the phosphor are agglomerated with irregular shapes. The surface of the SEM micrograph shows lots of voids and pores due to the large amount of gases such as NO_2 and CO_2 that evolve during combustion method [9]. Figure 3(b) shows the energy dispersive X-ray spectroscopy (EDS) spectrum of $\text{BaB}_8\text{O}_{13}:0.05\text{Ce}^{3+}$ powder phosphor. The spectrum confirms the presence of barium (Ba), Boron (B), oxygen (O) and Cerium (Ce) elements. The concentration of Ba by weight exceeds those of all the other elements and the least concentration (also by weight) was recorded for Ce^{3+} used as a dopant.

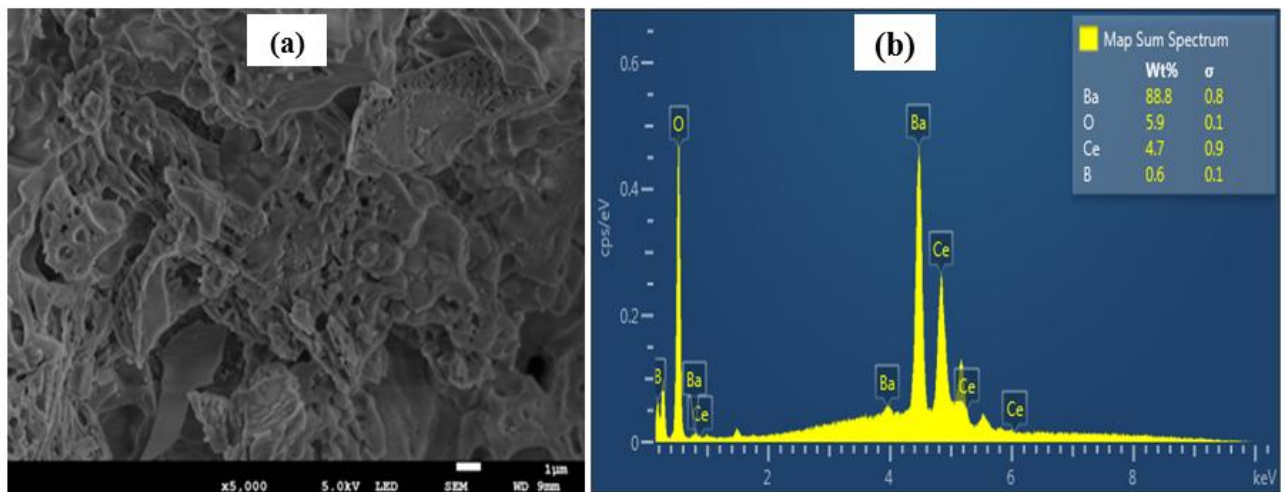


Figure 3. (a) SEM micrograph and (b) EDS spectrum of $\text{BaB}_8\text{O}_{13}:0.05\text{Ce}^{3+}$ phosphor.

Figure 4(a) shows the photoluminescence excitation (PLE) of $\text{BaB}_8\text{O}_{13}:0.05\text{Ce}^{3+}$ phosphor and photoluminescence emission (PL) spectra of $\text{BaB}_8\text{O}_{13}:x\text{Ce}^{3+}$ ($x = 0.03, 0.05, 0.07, 0.09$ and 0.11) powder phosphors. The PLE spectrum consists of a major peak centered at 270 nm and a minor peak at 212 nm due to the $4f^1 - 5d^1$ excitation transition of Ce^{3+} ions and the excitonic band, respectively

[10]. The feature of the excitation spectrum remains the same when monitored using 515 nm emission peak indicating that the emission obtained is due to same recombination center [11]. When exciting the $\text{BaB}_8\text{O}_{13}:x\text{Ce}^{3+}$ ($x = 0.03, 0.05, 0.07, 0.09$ and 0.11) powder phosphors at 270 nm wavelength, a broad emission peak was observed at 515 nm, which is attributed to the inter-configuration $5d^1 - 4f^1$ allowed transition of Ce^{3+} [9, 12]. The concentration of Ce^{3+} versus relative emission intensity plot of $\text{BaB}_8\text{O}_{13}$ doped with different concentrations of Ce^{3+} under 270 nm excitation is shown as an inset in figure 4(a). The plot shows PL intensity increased with concentration from 0.03 and maximizes at 0.05 mol beyond which the PL intensity decreased. The decrease in the PL emission intensity beyond the critical concentration could be explained by concentration quenching effect. The probability of energy transfer is greatly dependent on the distance between the activator ions. As the Ce^{3+} doping amount increases the distance between Ce^{3+} ions shortens, which favors the non-radiative pathway by energy transfer among Ce^{3+} ions [13]. Generally, the emission of Ce^{3+} has a doublet character with an energy difference of about 2000 cm^{-1} due to the ground-state splitting (${}^2\text{F}_{5/2}$ and ${}^2\text{F}_{7/2}$) [14]. To confirm this, the PL spectrum of $\text{BaB}_8\text{O}_{13}:0.05\text{Ce}^{3+}$ (figure 4(b)) was deconvoluted into two Gaussian profiles with peaks centered at 508 nm (19685 cm^{-1}) and 551 nm (18149 cm^{-1}). The energy difference (Δk) between them is about 1536 cm^{-1} , which shows a small difference compared with the theoretical value of 2000 cm^{-1} . This indicates that there is only one type of emission center in the $\text{BaB}_8\text{O}_{13}$ host lattice [15].

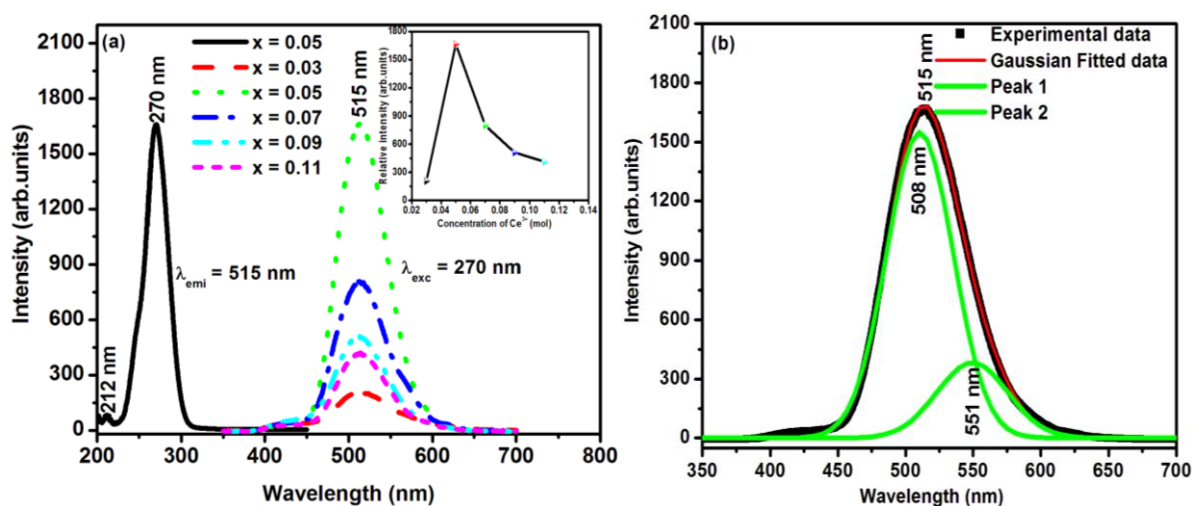


Figure 4. (a) Excitation spectrum of $\text{BaB}_8\text{O}_{13}:0.05\text{Ce}^{3+}$ and emission spectra of $\text{BaB}_8\text{O}_{13}:x\text{Ce}^{3+}$ ($x = 0.03, 0.05, 0.07, 0.09$ and 0.11) powder phosphors, with relative intensity versus concentration of Ce^{3+} as an inset and (b) deconvoluted emission spectrum of $\text{BaB}_8\text{O}_{13}:0.05\text{Ce}^{3+}$ powder phosphor.

The Commission International de l'Eclairage (CIE) 1931 Chromaticity image for $\text{BaB}_8\text{O}_{13}:x\text{Ce}^{3+}$ ($x = 0.03, 0.05, 0.07, 0.09$ and 0.11) phosphor powders excited at 270 nm is shown in figure 5. The CIE coordinate values were found to be (0.243, 0.481), (0.190, 0.572), (0.200, 0.536), (0.192, 0.503) and (0.209, 0.536) for $x = 0.03, 0.05, 0.07, 0.09$ and 0.1 , respectively. The CIE coordinates are in the green region of the spectrum not far from the standard green phosphor with the coordinates (0.31, 0.60), which means this phosphors can be used as a source of green light in many light emitting devices of different types.

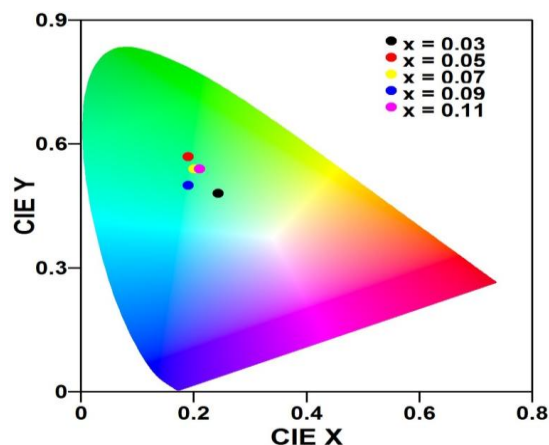


Figure 5: CIE chromaticity diagram of BaB₈O₁₃ doped different concentrations of Ce³⁺.

Conclusion

A detailed synthesis of a series of Ce³⁺ activated BaB₈O₁₃ powder phosphors using the combustion method was presented. The phosphors were evaluated for a possible application as a source of green light in light emitting devices. The XRD patterns of the phosphors were found to be consistent with the standard orthorhombic crystal structure of BaB₈O₁₃. The photoluminescence spectroscopy data showed a broad emission centered at 515 nm under the UV excitation of 270 nm. The PL emission intensity was dependent on the concentration of Ce³⁺ with the maximum concentration obtained from the 0.05 mol Ce³⁺ doping. The CIE chromaticity coordinates indicated that the Ce³⁺ doped phosphors exhibit a green color, with coordinates close to those of the standard green phosphor, suggesting that our material is a potential candidate to be used as source of green light in different types of light emitting devices.

Acknowledgements

The authors would like to acknowledge financial assistance from the National Research Foundation (NRF), South Africa: (grants no: AEMD160523165935, SFH13081628745, 93936 and UID. 99378).

References

- [1] Zhang J, Han B, Zhang Y and Lv Q 2016 *J. Mater. Sci: Mater Electron.* **27** 3906
- [2] Lephoto M A, Tshabalala K G, Motloung S J, Ahemen I and Ntwaeaborwa O M 2017 *PhyB*. doi.org/10.1016/j.physb.2017.06.063.
- [3] Malchukova E and Boizot B 2014 *J Rare Earth.* **32** 217
- [4] Lee S, Huang C, Chan T and Chen T 2014 *Appl. Mater. Interface.* **6** 7260
- [5] Devaraja P B, Avadhani D N, Nagabhusana H, Prashantha S C, Sharma S C, Nagabhusana B M, Nagaswarupa H P and Prasad B D 2015 *J. Radiat. Res. Appl. Sci.* **8** 362
- [6] Mothudi B M, Ntwaeaborwa O M, Shreyas S Pitale, Swart H C 2010 *J. Alloys. Compd.* **508** 262
- [7] Chenari H M, Moafi H F and Rezaee O 2016 *Mater. Res.* **19** 548
- [8] Tamrakar R K and Dubey V 2016 *J. Taibah Univ. Sci.* **10** 317
- [9] Dhananjaya N, Nagabhushana H, Nagabhushana B M, Rudraswamy B, Shivhakumara C and Chakradhar R 2012 *Bull. Mater. Sci.* **35** 519
- [10] Pawade V B, Dhoble N S and Dhoble S J 2015 *Mater. Res. Express.* **2** 095501
- [11] Weon G S, Miso P, Jinhyoung K, Sang W J, Insu C, Youngku S 2014 *Thin Solid Films* **565** 293
- [12] Sharma S K, Pitale S S, Malik M M, Dubey R N and Qureshi M S 2009 *J. Lumin.* **129** 140
- [13] Chen Y, Cheah K W and Gong M 2011 *J. Lumin.* **131** 1589
- [14] Zhong J, Zhuang W, Xing X, Liu R, Li Y, Liu Y and Hu Y 2015 *J. Phys. Chem. C* **119** 5562
- [15] Zhou J, Xia Z, Yang M and Shen K 2012 *J. Mater. Chem.* **22** 21935